Biochemistry **1980**, *19*, 2491–2497

Gresser, I., Brouty-Boyé, D., Thomas, M., & Macieira-Coelho, A. (1970) *Proc. Natl. Acad. Sci. U.S.A. 66*, 1052–1058.

Grossberg, S. E., Smith, A. J., & Sedmak, J. J. (1975) in *Effects of Interferon on Cells, Viruses, and the Immune System* (Geraldes, A., Ed.) Academic Press, London.

Jankowski, W. J., Von Meunchhausen, W., Sulkowski, E., & Carter, W. A. (1976) *Biochemistry 15*, 5182–5187.

Kerr, I. M., & Brown, R. E. (1978) *Proc. Natl. Acad. Sci. U.S.A. 75*, 256–260.

Kohase, M., & Vilček, J. (1977) *Virology 76*, 47–54.

Lab, M., & Kochran, F. (1972) *Ann. Inst. Pasteur, Paris 122*, 569–573.

Nilsen, T. W., & Baglioni, C. (1979) *Proc. Natl. Acad. Sci. U.S.A. 76*, 2600–2604.

Pfeffer, L. M., Murphy, J. S., & Tamm, I. (1979) *Exp. Cell Res. 121*, 111–120.

Pitha, P. M., & Carter, W. A. (1971) *Virology 45*, 777–781.

Sehgal, P. B., Tamm, I., & Vilček, J. (1976a) *Virology 70*, 256–259.

Sehgal, P. B., Tamm, I., & Vilček, J. (1976b) *Virology 70*, 532–541.

Sehgal, P. B., Tamm, I., & Vilček, J. (1976c) *Science 190*, 282–284.

Sehgal, P. B., Dobberstein, B., & Tamm, I. (1977) *Proc. Natl. Acad. Sci. U.S.A. 74*, 3409–3413.

Sehgal, P. B., Lyles, D. S., & Tamm, I. (1978) *Virology 89*, 186–198.

Slate, D. L., & Ruddle, F. H. (1979) *Cell 16*, 171–180.

Stewart, W. E., II (1979) *The Interferon System*, Springer-Verlag, New York.

Tan, Y. H., Armstrong, J. A., Ke, Y. H., & Ho, M. (1970) *Proc. Natl. Acad. Sci. U.S.A. 67*, 464–481.

Tomkins, G. M., Gelenhiter, T. D., Granner, D., Martin, D., Samuels, H. H., & Thompson, E. B. (1969) *Science 166*, 1474–1480.

Vilček, J., & Ng, M. H. (1971) *J. Virol. 7*, 588–594.

Vilček, J., & Havell, E. A. (1973) *Proc. Natl. Acad. Sci. U.S.A. 70*, 3909–3913.

Conformational Flexibility of the 3′ Acceptor End of Transfer Ribonucleic Acid[†]

D. M. Cheng, S. S. Danyluk, M. M. Dhingra,[‡] F. S. Ezra,[§] M. MacCoss, C. K. Mitra, and Ramaswamy H. Sarma*

ABSTRACT: The intimate details of the conformational features and dynamics of the trinucleoside diphosphates CpCpA and ApCpC in aqueous solution have been arrived at by the complete analysis of their proton magnetic resonance spectra. In addition to the right-handed stacked species in which the phosphodiester torsions conform to the gauche–gauche domains, sugar puckers ^{3}E, C4′–C5′ $\simeq$ 60°, C5′–O5′ $\simeq$ 180°, C3′–O3′ $\simeq$ 205°, and $\chi_{CN} \simeq 40°$, the trimers display a variety of spatial configurations, an important one being a bulged configuration in which the central nucleotide unit is bulged out, enabling stacking interactions between the end units. It is further shown that the 3′ acceptor end of tRNA, CpCpA, displays considerable flexibility for the terminal adenine nucleotide unit. Theoretical NMR calculations demonstrate that the predominant solution conformation does not conform to the CCA terminus of tRNA as reported by four independent crystallographic studies of tRNA^{Phe}. It is shown that the preferred intramolecular order of CCA in solution is such that $\chi_1 = \chi_2 = \chi_3 = 40°$, all the three sugars are in ^{3}E, $\psi_1 = \psi_2 = \psi_3 = 60°$, ϕ_2 and ϕ_3 = 170 and 180°, respectively, $\phi_1' = \phi_2' = 205°$, and ω_1/ω_1' and ω_2/ω_2' = 240/205° and 295/265°, respectively.

The ubiquitous presence of the sequence CpCpA at the 3′ acceptor end of tRNA has been known for a long time. Less is known about geometric features in solution of this unique trinucleotide and the possible role in recognition of a variety of aminoacyl-tRNA synthetases. In an attempt to approach this problem from a structural perspective, we have investigated the conformational properties of CpCpA and ApCpC in aqueous solution, and we report our findings in this paper.

Comprehensive investigations of the conformational properties of ribodinucleoside monophosphates in aqueous solution (Lee et al., 1976; Ezra et al., 1977; Dhingra et al., 1978) have provided information about the stereochemical principles involved in the 3-D topology of these molecules. These studies revealed the presence of a coupled set of base sequence dependent conformational parameters and interdependent structural changes linked to base stacking interactions (Lee et al., 1976; Ezra et al., 1977; Dhingra et al., 1978; Evans & Sarma, 1976; Sarma & Danyluk, 1977; Cheng & Sarma, 1977). A natural extension is the investigation of the spatial configuration and conformational properties of higher oligomers. However, the higher oligomers have presented a difficult problem with respect to the complete analysis of their ^{1}H spectra. Selective deuteration studies (Kondo et al., 1975) enabled unambiguous assignment of the H1′ of each of the residues of ApApA. Computer-assisted analysis enabled Evans & Sarma (1976) to determine the signals which are coupled to each other in each of the residues in ApApA even though an unambiguous assignment of each of the protons by this method is not possible. A complete unambiguous assignment

---

[†] From the Institute of Biomolecular Stereodynamics and Department of Chemistry, State University of New York at Albany, Albany, New York 12222 (D.M.C., M.M.D., C.K.M., and R.H.S.), and the Division of Biological and Medical Research, Argonne National Laboratory, Argonne, Illinois 60439 (S.S.D., F.S.E., and M.M.). *Received December 7, 1979.* This work was supported by Grant CA12462 from the National Cancer Institute, Department of Health, Education, and Welfare, Grant PCM75-16406 from the National Science Foundation, Grant 1-P07-PR00798 from the Division of Research Sources, National Institutes of Health, and the U.S. Department of Energy.

[‡] Present address: Tata Institute of Fundamental Research, Bombay 400 005, India.

[§] Present address: Miami Valley Laboratories, Proctor and Gamble Corp., Cincinnati, OH 45247.

0006-2960/80/0419-2491$01.00/0

Table I: Chemical Shifts in ppm (Top) and Coupling Constants in Hertz (Bottom) for the Trimers

nucleotide		T (°C)	1′	2′	3′	4′	5′	5″	Δ5′5″	H2 (H5)	H8 (H6)
ApCpC:	Ap-	19	2.838	1.676	1.433	1.271	0.741	0.892	0.151	4.931	5.159
	-pCp-		2.415	1.096	1.265	1.211	1.251	0.899	0.352	2.362	4.453
	-pC		2.666	0.921	1.076	1.029	1.099	0.973	0.126	2.685	4.667
ApCpC:	Ap-	80	2.882	1.666	1.573	1.265	0.698	0.782	0.084	5.054	5.133
	-pCp-		2.711	1.163	1.403	1.248	1.141	1.079	0.062	2.712	4.599
	-pC		2.743	0.973	1.031	1.061	1.104	1.000	0.104	2.831	4.658
CpCpA:	Cp-	19	2.527	1.278	1.374	1.111	0.687	0.836	0.149	2.598	4.629
	-pCp-		2.608	1.143	1.374	1.204	1.201	0.984	0.220	2.482	4.606
	-pA		2.937	1.337	1.335	1.143	1.184	0.984	0.200	5.048	5.329
CpCpA:	Cp-	70	2.691	1.082	1.374	1.015	0.612	0.707	0.095	2.714	4.577
	-pCp		2.618	1.152	1.284	1.024	0.984	0.896	0.088	2.714	4.531
	-pA		2.901	1.465	1.284	1.152	1.034	0.954	0.080	5.055	5.215

nucleotide		T (°C)	1′2′	2′3′	3′4″	4′5′	4′5″	3′P	4′P	5′P	5″P	5′5″	56
ApCpC:	Ap-	19	2.8	4.7	7.0	2.2	3.6	9.0				−13.0	
	-pCp-		2.2	4.8	7.6	2.0	1.8	8.5	2.0	4.0	2.8	−12.0	7.5
	-pC		3.4	4.9	6.5	2.4	3.2		1.9	3.2	4.3	−12.0	7.5
ApCpC:	Ap-	80	5.0	4.7	4.8	3.0	4.0	7.8				−13.0	
	-pCp-		4.2	4.9	5.7	2.0	3.0	8.0	3.0	2.6	5.4	−11.4	7.5
	-pC		4.0	4.5	5.8	4.8	3.6		2.5	5.6	4.5	−11.2	7.5
CpCpA:	Cp-	19	2.8	5.4	6.9	2.3	3.5	8.5				−12.7	7.6
	-pCp-		2.3	5.5	7.3	2.4	2.3	8.0		3.2	4.2	−12.0	7.6
	ppA		4.6	5.2	5.4	2.9	3.6		2.1	3.7	3.9	−11.8	
CpCpA:	Cp-	70	4.5	5.2	5.5	3.0	4.3	8.3				−12.6	7.6
	-pCp-		3.7	5.4	6.0	2.6	3.1	7.7		3.8	4.3	−12.2	7.7
	-pA		5.6	5.3	4.3	3.1	4.0		2.4	4.1	4.8	−11.5	

for ApApA has been reported elsewhere (Dhingra & Sarma, 1979). Recently, through a combination of hetero- and homonuclear decoupling experiments and computer simulations, we arrived at complete assignments of the deoxytrimers dTpTpT and dTpTpC (Cheng et al., 1978). In this paper we report the analysis of high-field ^{1}H NMR spectra and the conformational deductions for the trinucleoside diphosphates CpCpA and ApCpC. The results show that CpCpA (and by inference the 3′ acceptor end of tRNA) can adopt a variety of spatial configurations with considerable flexibility for the terminal adenine nucleotide unit.

Experimental Section

A mixture of cytidine 2′,5′- and 3′,5′-diphosphates was synthesized from cytidine by a modification of the procedure of Hall & Khorana (1955) using phosphorus pentoxide and 85% orthophosphoric acid. A significant increase in yield was obtained by carrying out the reaction under a stream of dry N_2. The products were separated by the method of Verheyden & Moffat (1964) followed by purification on a Whatman DE-52 cellulose column (HCO_3^- form, eluting with a linear gradient of ammonium bicarbonate). The ^{1}H NMR spectrum showed the product to be a 60:40 mixture of cytidine 3′,5′-diphosphates in addition to a trace amount (<5%) of the cytidine diphosphate in the arabino configuration. Cytidine 3′,5′-diphosphate was prepared from the mixture by the procedure of Michelson (1966) using ethyl chloroformate and tri-*n*-butylamine in H_2O to produce cytidine cyclic 2′,3′-phosphate 5′-phosphate ethyl carbonate anhydride. The cyclic 2′,3′-phosphate moiety was enzymatically cleaved by using ribonuclease in 0.05 M tris(hydroxymethyl)aminomethane at pH 6.8 and room temperature. Alkaline hydrolysis at pH 13 for 4 h gave cytidine 3′,5′-diphosphate. Final purification was carried out on a Whatman DE-52 column (HCO_3^- form) using a linear gradient of ammonium bicarbonate (pH 8.0) as elutant.

The trinucleoside diphosphates CpCpA and ApCpC were purchased from Sigma Chemical Co. in the acid or the salt form. The samples were lyophilized 3 times from 99.8% D_2O, and the final solutions were made up with 100% D_2O. The pD values of the solutions were adjusted to 7.4 for the trimers and 5.5 for 3′,5′-CDP. Final concentrations were estimated to be ~0.01 M.

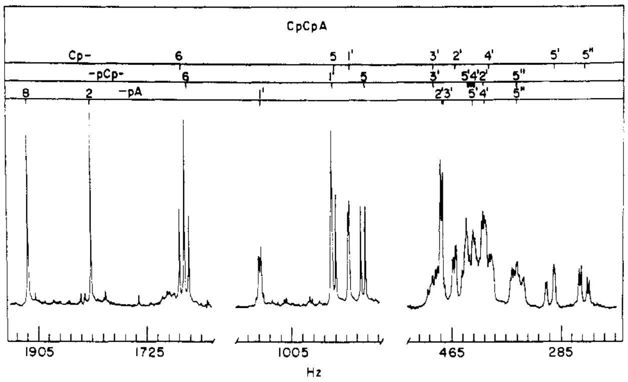

FIGURE 1: 360-MHz ^{1}H NMR spectrum of CpCpA in D_2O, pD 7.4 at 19 °C. The shifts are given in hertz (at 360 MHz) relative to internal tetramethylammonium chloride.

Proton spectra were recorded in the FT ^{1}H, ^{1}H{^{1}H}, and ^{1}H{^{31}P} modes on Varian 220-, Bruker 270-, and Bruker 360-MHz NMR spectrometers by using tetramethylammonium chloride (TMA) as an internal reference.

Results and Discussion

Assignments and Analysis. Assignments were made by extensive proton–proton and proton–phosphorus decoupling experiments, by comparison of the spectra with the constituent monomers and dimers, and by extensive computer simulation. We have discussed elsewhere (Cheng et al., 1978) in detail the methodology involved in the assignment of the resonances in trinucleosides. In Figure 1 is illustrated the complete 360-MHz spectrum (along with the assignments) of CpCpA. Figure 2 displays the high-field region of ApCpC along with the simumation of the Ap-, -pCp-, and -pC segments as well as the complete simulation. Because of the extensive overlap in certain regions, errors of as much as 0.4 Hz (and hence up to 5% error in populations, Table II) may be involved in some coupling constants. The chemical shift and coupling constant data are summarized in Table I; the shifts are accurate to

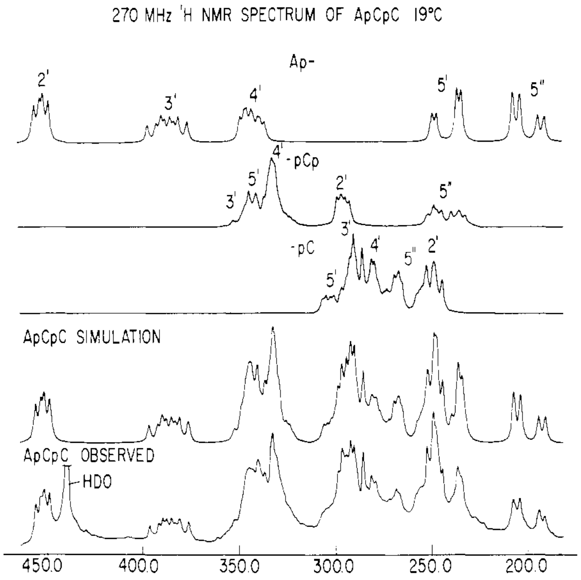

FIGURE 2: Observed (lower trace) and computer-simulated high-field region of the 270-MHz ^{1}H NMR spectra of ApCpC at 19 °C. The shifts are in hertz (270-MHz system) relative to internal tetramethylammonium chloride. The simulation was done by using the standard LACOON III program.

0.001 ppm, and the effect of 0.001-ppm error in shifts on calculations presented later is negligible.

Local Conformational Properties. A complete description of the spatial configuration of a trinucleoside diphosphate involves the determination of the conformation of three ribose rings and the specification of 14 torsion angles. The IUPAC–IUB nomenclature employed is illustrated in Figure 3. The conformational details were calculated from coupling constants by using procedures presented elsewhere (Lee et al., 1976). The calculated conformations for CpCpA and ApCpC along with those for the constituent dimers and monomers are given in Table II, and the error limitations are discussed elsewhere by Lee et al. (1976).

The ribose coupling constants in both trimers can be explained in terms of a $^2E \rightleftarrows {}^3E$ equilibrium (see Figure 3 for nomenclature) similar to that found for monomers and dimers (Lee et al., 1976; Ezra et al., 1977; Evans & Sarma, 1976). At 19 °C a preference is observed for the ^3E sugar pucker ranging from a minimum of 56% in the -pA fragment of CpCpA to a maximum of 78% in the -pCp- segment of ApCpC; also the central nucleotide unit has a higher preference for the ^3E mode compared with the outer residues in both trimers. It is further observed that the movement of adenine from the 5′-terminal end as in ApCpC to the 3′ end as in CpCpA causes noticeable reduction in the population of ^3E conformers for the -pA unit, so much so that the terminal ribose exists as a $^2E \rightleftarrows {}^3E$ equilibrium with roughly equal populations of both in the latter trimer. But comparison of the cytidine nucleotidyl terminal fragments shows that movement of cytidine from 5′ to 3′ ends (i.e., CpCpA → ApCpC) results in a much smaller shift for the $^2E \rightleftarrows {}^3E$ equilibrium. These are all indications of the flexbility associated with the -pA residue of CpCpA. An increase in the temperature from 19 to 70–80 °C causes a 10–30% decrease in the ^3E populations for the nucleotidyl fragments such that the $^2E/^3E$ blends are roughly 50:50 in the trimer at the higher temperature. Incorporation of the mononucleotide into the

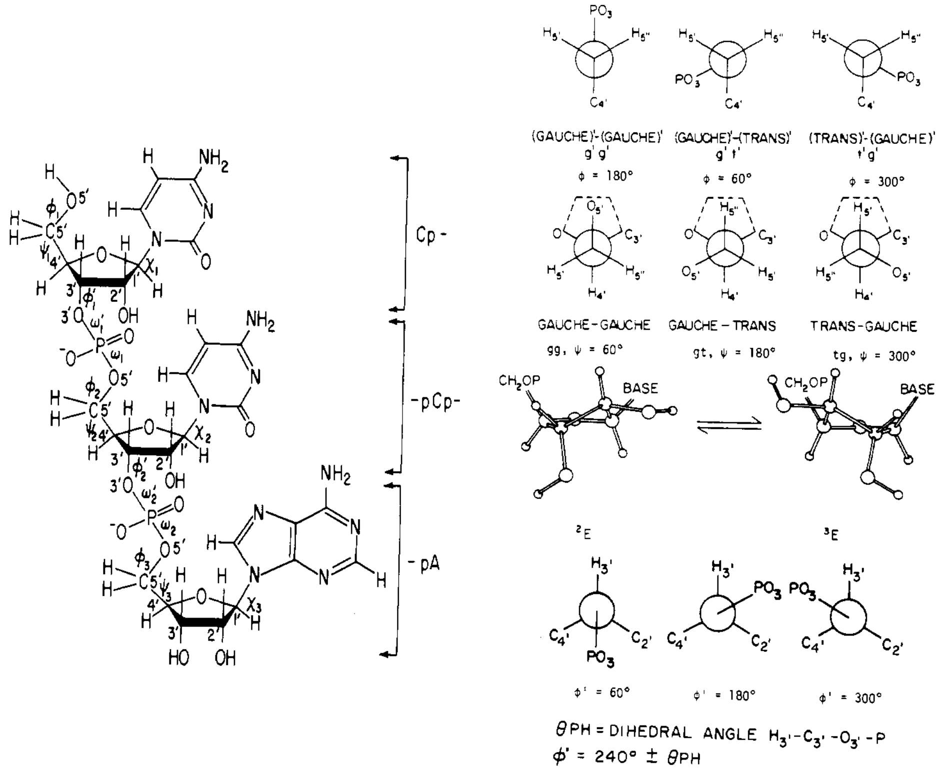

FIGURE 3: Structure and conformational nomenclature of CpCpA. Each bond in a nucleotide unit is represented by a greek letter, and numbers 1, 2, 3, etc. are used to designate the nucleotide unit. The torsion angles are the angles between two adjacent bonds when viewed along the central bond. The value is zero for a cis arrangement. Examination of the Newman projections on the right-hand side makes these definitions understandable. For the sugar ring two principal conformations are employed. In the C2′-endo form (^2E), C2′ is puckered (major pucker) in the same direction as C5′ (and the base) and the C1′, O4′ and C4′ lie in one plane. In the C3′-endo conformation (^3E), C3′ is puckered in the same direction as C5′ (and the base) and C1′, O4′, and C4′ again lie in one plane. In either case, C3′ (for C2′-endo) or C2′ (for C3′-endo) undergoes a minor pucker below the plane of C1′, O4′, and C4′ (i.e., opposite to the C5′ relative to the plane). These are the two major conformations for ribose that are energetically most stable and experimentally more commonly observed.

Table II: Population Distribution of Conformers in ApCpC and CpCpA in the Constituent Units

			trimer				dimer				monomer			
nucleotide		temp (°C)	% ^{3}E	ΘPH (deg)	% g',g'	% g,g	% ^{3}E	ΘPH (deg)	% g',g'	% g,g	% ^{3}E	ΘPH (deg)	% g,g'	% g,g
ApCpC:	Ap-	19	71	±32		81	64	±33		85	31	±36		82
	-pCp		78	±34	84	84			85	87	49	±34	74	90
	-pC		66		88	100	71		84	92	55		75	77
ApCpC:	Ap-	80	49	±37		69	44	±36		69				
	-pCp-		58	±36	82	90			70	69				
	-pC		59		72	55			70					
CpCpA:	Cp-	19	71	±34		81	74	±35		81	60	±35		71
	-pCp-		76	±36	85	100			84	85	49	±34	74	90
	-pA		56		86	74	56		84	90	40		72	77
CpCpA:	Cp-	70	57	±34		66	71	±35						
	-pCp		61	±37	82	80								
	-pA		45		78	64	57							

backbone framework of a dimer to form the trimer results in a substantial shift in the $^2E \rightleftarrows {}^3E$ equilibrium toward the ^{3}E mode (Table II). However, the major oligomerization change occurs at the first step in polymerization, i.e., monomer → dimer. This has been observed earlier by Evans & Sarma (1976).

The average dihedral angle about C3′–O3′ (ΘPH = 0° when $\phi' = 240°$, Figure 3) at 19 °C in CpCpA and ApCpC was found to be (Table II) ±34° (ϕ_1' and $\phi_2' \simeq 206$ and/or 274°). No significant difference is observed between ϕ_1' and ϕ_2'. Because of the conformational interrelationship (Lee et al., 1976; Dhingra et al., 1978; Evans & Sarma, 1976; Sarma & Danyluk, 1977) between the ribose ring pucker and the orientation of the C3′–O3′ bond, the domain centered around $\phi' \simeq 206°$ is associated with ^{3}E and that around $\phi' \simeq 274°$ is associated with ^{2}E. Since CpCpA and ApCpC prefer a ^{3}E pucker, the preferred orientation for C3′–O3′ in both systems is around ϕ_1' and $\phi_2' \simeq 206°$. Temperature variation or oligomerization apparently has little effect on the magnitude of ϕ'. However, it should be noted that lowering of temperature and oligomerization causes shifts of the $^2E \rightleftarrows {}^3E$ equilibrium toward ^{3}E and hence under these conditions the C3′–O3′ bond will increasingly occupy the $\phi' \simeq 206°$ domain.

The C4′–C5′ and C5′–O5′ bonds show an overwhelming preference for g,g (ψ_1, ψ_2, and $\psi_3 = 60°$, Figure 3) and g',g' (ϕ_2 and $\phi_3 = 180°$, Figure 3) conformations, respectively. As has been noted for dinucleoside monophosphates (Lee et al., 1976; Ezra et al., 1977; Dhingra et al., 1978), elevation of temperature causes a reduction in these gauche–gauche populations. A progression from dimer to trimer produces several interesting local changes (Table II). Thus, in going from ApC to ApCpC no change occurs about ψ_1 and ψ_2 but from CpC to CpCpA the $\psi_2 = 60°$ population increases; from CpA to CpCpA there is a reduction in the population of $\psi_3 = 60°$ conformers, again suggesting the flexibility at the 3′ end (vide supra) for a purine nucleotidyl unit.

The difficulty in arriving at quantitative information about the sugar–base torsion angle (χ) by NMR measurements has been discussed in extenso elsewhere (Lee et al., 1976; Ezra et al., 1977; Dhingra et al., 1978). As in the earlier work, the preponderance of shift evidence favors a sugar–base torsion in the anti domain. It has been shown (Lee et al., 1976; Ezra et al., 1977; Dhingra et al., 1978; Evans & Sarma, 1976; Sarma & Danyluk, 1977) that the $^2E \rightarrow {}^3E$ shift is associated with a reduction in the magnitude of χ in the anit domain. The present observation that upon oligomerization (monomer → dimer → trimer) the sugar ring shifts increasingly toward ^{3}E suggests that in the trimers the magnitude of χ approaches smaller values (vide infra).

Intramolecular Order in ApCpC. Trimerization shifts for H5 and H6 of the central -pCp- unit indicate that they have shifted to high field by 0.595 and 0.396 ppm (see supplementary material paragraph at end of paper for Table III), suggesting stacking interactions between adjacent bases. A normally preferred stacked arrangement for nucleic acids is the one in which the phosphodiester bonds exist in g^-,g^- ($\omega \simeq 290°$ and $\omega' \simeq 290°$) domains. We have discussed elsewhere (Lee et al., 1976; Ezra et al., 1977; Dhingra et al., 1978) that a g^-,g^- arrangement will result in the deshielding of the interior H5′ by the 2′-OH of the nucleotide unit at the 5′ end. The data show that in the ApCp- segment of ApCpC, the interior H5′ is deshielded by 0.296 ppm, clearly suggesting the dominant stacked array for the ApCp- segment to be g^-,g^-. Comparison of the shift data for the interior H5′ of ApC with that of the ApC- segment of ApCpC suggests that the population of conformers in which ω_1,ω_1' is g^-,g^-, is larger in the trimer compared to that in ApC. *The oligomer shift data for the interior H5′ of CpC and the -CpC segment of ApCpC clearly suggest the presence of detectable populations in which ω_2',ω_2 occupies g^-,g^- domains but the g^-,g^- populations about ω_2',ω_2 have decreased compared to that in CpC.* Such an observation of the population of g^-,g^--stacked arrays in the -CpC segment of the trimer apparently seems to contradict the observation that the H5 and H6 of the -pC part of ApCpC have shifted substantially to higher fields compared to the -pC segment of CpC, i.e., 0.255 vs. 0.166 ppm for H5 and 1.169 vs. 0.099 ppm for H6. Even though such shifts may be rationalized on the basis of changes in χ_{CN} or changes in relative geometry between the adjacent cytosine rings in the trimer compared to that in the dimer, because of the smaller deshielding abilities of cytosine and because of the observation of the decrease in the population of stacked g^-,g^- arrays about ω_2',ω_2, a likely explanation for this is due to the presence of small percentages of spatial configurations in which the central cytidine in ApCpC is bulged out, enabling stacking interactions between the terminal adenine and cytosine systems. This is not surprising because such bulged configurations have been found for dApTpT and dTpTpA (Cheng et al., 1978). The next nearest neighbor NMR data reported by Bell and Nielson and their co-workers (Everett et al., 1980) also support bulged configurations in ApGpX and CpApX systems.

Intramolecular Order in CpCpA. The chemical shifts of H5 and H6 of the central -Cp- residue have been shifted to higher fields by 0.475 and 0.243 ppm, respectively, in CpCpA, indicating stacking interactions between the adjacent bases. The data show that in the CpCp- segment of CpCpA, the interior H5′ is deshielded by 0.206 ppm, clearly suggesting that the dominant stacked array for the CpCp- segment is g^-,g^-. Comparison of the shift data for the interior H5′ of CpC with those of the CpC- segment of CpCpA suggests that the

Table IV: Chemical Shifts (ppm) of the CCA Residue for Various Conformations[a]

							soln conf		
no.	proton	DUKE	MSN	MRC	MIT	α-RNA-11	calcn no. 1	calcn no. 2	exptl[b]
1	H1′ (C1)	*0.23*	*−0.01*	*0.04*	*0.08*	*0.14*	*0.13*	*0.26*	0.219
2	H2′ (C1)	0.20	0.02	0.17	−0.03	0.10	0.06		−0.051
3	H3′ (C1)	0.23	−0.02	−0.02	−0.01	−0.07	0.10		−0.028
4	H4′ (C1)	0.07	−0.03	−0.04	0.00	−0.04	0.04		−0.017
5	H5′ (C1)	0.06	−0.01	−0.02	0.00	−0.03	0.04		−0.033
6	H5″ (C1)	0.08	−0.02	0.00	0.00	−0.02	0.04		−0.094
7	H5 (C1)	*0.07*	*−0.02*	*−0.05*	*0.55*	*−0.05*	*0.14*	*0.26*	0.280
8	H6 (C1)	*0.01*	*−0.03*	*−0.06*	*0.14*	*−0.02*	*0.14*	*0.16*	0.065
9	H1′ (C2)	*0.12*	*0.01*	*0.03*	*0.25*	*0.16*	*0.24*	*0.26*	0.205
10	H2′ (C2)	0.00	−0.03	0.03	0.02	−0.24	0.05		0.077
11	H3′ (C2)	0.09	−0.03	0.00	0.00	−0.13	0.08		0.080
12	H4′ (C2)	0.14	−0.02	−0.03	0.10	−0.05	0.02		0.057
13	H5′ (C2)	0.13	−0.02	−0.07	0.11	−0.05	−0.03		−0.260
14	H5″ (C2)	0.12	−0.03	−0.02	0.11	−0.08	0.00		−0.055
15	H5 (C2)	*0.25*	*0.11*	*0.49*	*0.12*	*0.77*	*0.31*	*0.43*	0.475
16	H6 (C2)	*0.14*	*0.01*	*0.05*	*0.58*	*0.19*	*0.26*	*0.28*	0.243
17	H1′ (A)	*0.00*	*0.00*	*−0.02*	*0.00*	*0.06*	*0.06*	*−0.03*	−0.006
18	H2′ (A)	0.01	0.00	−0.02	0.00	0.04	0.03		0.212
19	H3′ (A)	0.00	0.01	−0.03	0.01	0.04	0.05		−0.030
20	H4′ (A)	0.02	0.03	−0.05	0.03	0.05	0.00		0.045
21	H5′ (A)	0.01	0.05	−0.09	0.04	0.01	−0.05		−0.055
22	H5″ (A)	0.00	0.02	−0.05	0.04	−0.03	0.00		−0.255
23	H2 (A)	*−0.02*	*0.00*	*0.00*	*0.01*	*−0.01*	*0.02*	*−0.05*	0.000
24	H8 (A)	*0.00*	*0.00*	*−0.02*	*0.01*	*0.38*	*0.17*	*0.00*	−0.040

[a] Relative to the corresponding proton shifts in the monomer taken as zero. The X-ray data for tRNA are at 3.5-Å resolution. [b] Reproduced from Table III for comparison only.

population of conformers in which $\omega_1{}',\omega_1 = g^-,g^-$ is larger in the trimer compared to that in the dimer. Similar treatment of the data for the -CpA segment of CpCpA indicates that the dominant stacked array is also g^-,g^- and that the population of the g^-,g^- conformers about $\omega_2{}',\omega_2$ has increased compared with the dimer CpA. However, this increase in g^-,g^- population is not reflected in the base proton shifts because cytosine has relatively poor ring current fields. A structure of CpCpA in which $\omega_1{}',\omega_1$ and $\omega_2{}',\omega_2$ correspond to the g^-,g^- domains and other torsions conform to the preferred ones as given in Table II is shown in Figure 4f. It is not possible to state unequivocally that this is the dominant conformation for CpCpA in aqueous solution because a wide variety of solution state conformations contribute to the conformational blend and no reliable methodology exists to calculate the fraction of each conformer for *the trimers as a whole*. However, in suggesting that the conformation in Figure 4f may be the dominant one for CpCpA, we rely on the local conformational properties of the various segments of the trimer (Table II) and assume that these *properties are persistent*. In Figure 4f, the sugar rings are ^{3}E and ψ_1, ψ_2, and ψ_3 = 60° (*g,g*). The data for the Cp-segment of CpCpA indicate that % ^{3}E = 70 and % *g,g* = 80. This also means that % ^{2}E = 30 and % *g,t* = 20. We assume that in the trimer a majority of fractions which display ^{3}E sugar conformations also display *g,g* conformations about the various C4′–C5′ bonds. Similar assumptions are employed with respect to the interrelationships among the fractions of conformers about the various bonds in order to predict the dominant spatial configuration for the trimer as a whole.

It is of interest to examine whether the observed NMR shift data reported in Table III ($\Delta\delta_t$, see supplementary material) are in general agreement with any of the four reported crystal structures for the CCA terminus of tRNA or whether CCA in solution conforms to an α-RNA-11 structure (Arnott et al., 1969). For this purpose, the projected shielding constants for the base and sugar protons of the DUKE, MSN, MRC, and MIT (Sussman & Kim, 1976; Stout et al., 1976; Ladner et al., 1975; Quigley et al., 1975) and α-RNA-11 (Figure 4) models were computed by taking into consideration the contributions of ring current and diamagnetic and paramagnetic anisotropy terms by the methods described by Giessner-Prettre & Pullman (1976). The published *x*, *y*, and *z* values were used for the input coordinates, and the effects of the base of a given nucleotidyl unit on the protons of the remaining two nucleotidyl units were computed. X-ray data do not provide the atomic positions for the hydrogen atoms, and hence their positions were calculated from reasonable values of bond length, bond angles, and torsion angles. The anisotropy shifts due to the sugar and phosphate residues were ignored due to extreme complexity and the lack of availability of the shielding tensors from ab initio calculations. It should further be noted that the shifts of the sugar phosphate moiety remain approximately the same in going from monomer to trimer except for H5′ and H1′. We have elaborated elsewhere (Lee et al., 1976; Ezra et al., 1977) that H5′ of -pY in XpY is sensitive to the 2′-OH of Xp-. H1′ is obviously sensitive to the base because of its close proximity and hence to the value of χ. In a similar fashion, H6 (or H2) of the base is also influenced by the sugar and hence the shielding for H6 (or H2) is also χ dependent (Giessner-Prettre & Pullman, 1977, 1978).

The data are summarized in Table IV for the projected shieldings for the four crystal structures of the CCA terminus of tRNA^{Phe} as well as for the α-RNA-11 model for CCA. Comparison of the data with those obtained experimentally (Table IV) clearly indicates that CpCpA in aqueous soluton does not take up any of these five conformations (Figure 4).

A search in the various conformation domains of χ, ϕ, ϕ', ω, and ω' was made keeping sugar pucker at ^{3}E and ψ = 60° in order to arrive at the preferred intramolecular order of CpCpA in solution. The local domains for search were selected based upon NMR analysis. The torsion angles were varied at intervals of 5° until a reasonable agreement resulted between the calculated and observed shifts for the base protons and H1′. In the final derived conformation, the torsion angles are χ_1, χ_2, and χ_3 = 40°, sugar pucker = ^{3}E, ψ_1, ψ_2, and ψ_3 = 60°, ϕ_2 and ϕ_3 = 170 and 180°, respectively, $\phi_1{}'$ and $\phi_2{}'$

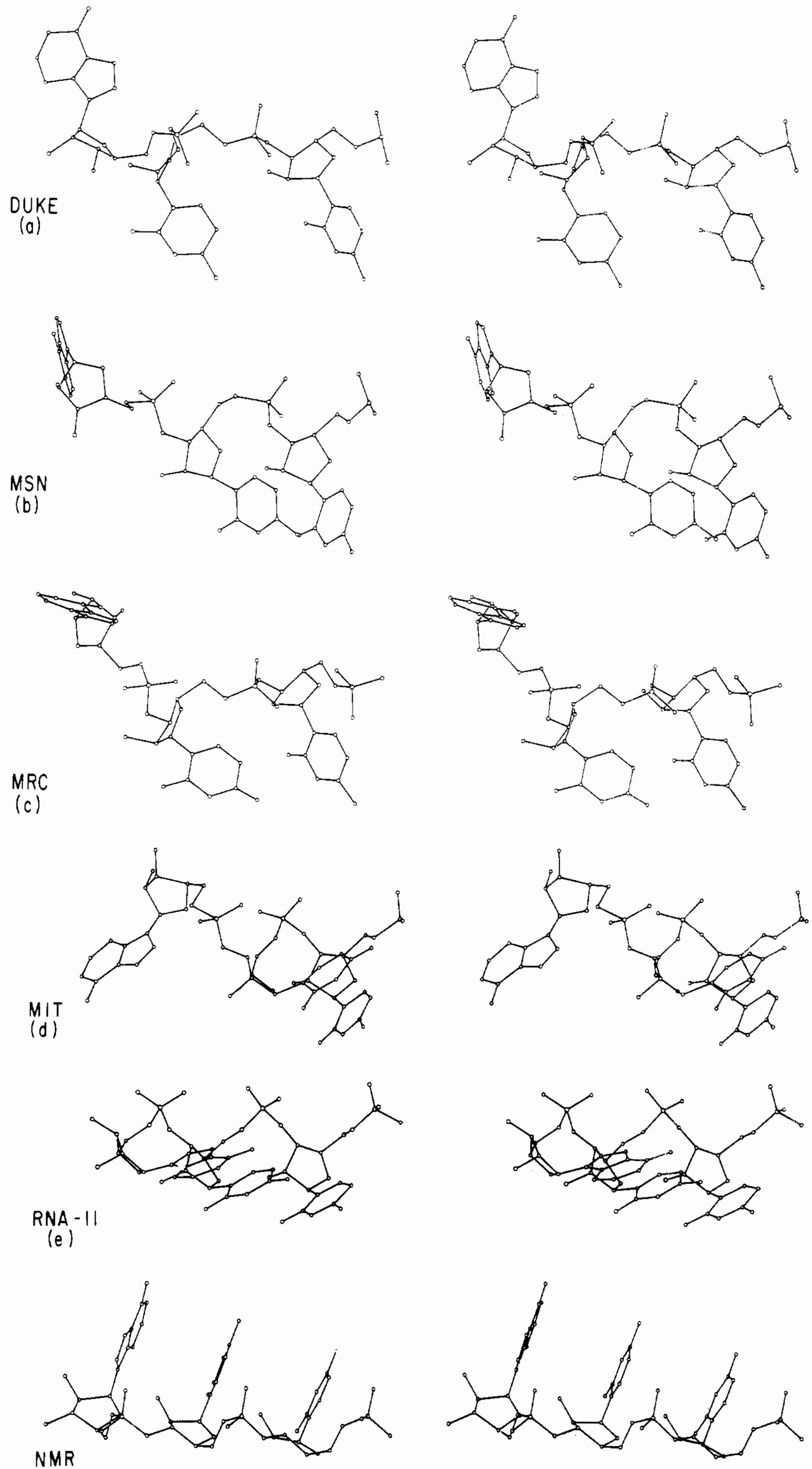

FIGURE 4: Stereographic drawings for the CCA terminus end of tRNA. (a)–(d) are the drawings for the CCA using the X-ray crystallographic coordinates from DUKE, MSN, MRC, and MIT data. (d) is the CCA molecule using Arnott's α-RNA-11 model geometry. (f) is the proposed NMR conformation (see text for conformation details). Hydrogen atoms have not been shown for clarity. The molecular orientation is the same in all six drawings; P(C1) and P(C2) are on the horizontal axis and P(A) is on the plane of the paper. A stereoscope is recommended for visualizing the drawings but is not essential.

= 205°, and ω_1/ω_1' and ω_2/ω_2' = 240/205° and 295/265°, respectively. A stereographic projection of CCA in this conformation is shown in Figure 4f. Table V (see supplementary material) lists in detail the contributions from ring current and diamagnetic and paramagnetic anisotropy effects to the projected shifts.

We have summarized in Table IV the finally calculated shifts (calculation no. 1) and the experimentally observed values. In view of the complexity involved, the agreement between the calculated and the observed values must be considered reasonable. However, some additional modifications of the calculated values are necessary to reflect the change of χ upon oligomerization because χ is assumed to be 40° in the monomers and the trimer and changes in χ upon oligomerization will definitely influence the projected shift changes of base protons and H1′. Hence, in Table IV (calculation no. 2) we have provided the projected shieldings for the base protons and H1′ for the CpCpA conformation shown in Figure 4f under conditions in which the value of χ in the cytidine monomer is 50° (90° for the adenine monomer) and those for the three χ values in CpCpA are equal to 40°. The agreement between the calculated and observed values is very good.

It is important to point out that the derived conformation for CpCpA (Figure 4f) is only the dominant one; in addition to this one, there can be minor contributions from other conformations, particularly a looped-out structure in which the central cytidine is bulged out, enabling stacking interactions between the bases of the end nucleotidyl units similar to those of dApTpT and dTpTpA (Cheng et al., 1978). It was pointed out that the population of $\psi_3 \simeq 60°$ conformers is noticeably less in CpCpA compared to CpA; movement of adenine from the 5′ end (i.e., ApCpC) to the 3′ end (i.e., CpCpA) shifts the $^2E \rightleftarrows {}^3E$ equilibrium toward ^2E so that the sugar ring of -pA of CpCpA displays equal proclivity for ^2E and ^3E conformations. Established conformational interrelationships (Lee et al., 1976; Ezra et al., 1977; Dhingra et al., 1978) have shown that in aqueous solution ^2E is associated with a $\phi' \simeq 274°$ and ^3E with a $\phi' \simeq 206°$ and in the anti domain χ_{CN} is larger for the ^2E system compared to ^3E. From these considerations, it is necessary to conclude that in addition to the spatial configuration depicted in Figure 4f, spatial configurations in which the geometric details of the adenosine moiety display considerable variation from other residues make contributions to the conformational blend. This conclusion is in eminent agreement with current views about nucleic acid statics and dynamics (Sarma, 1979; Neidle, 1979). Our observation that major conformational changes happen at the first step in oligomerization, i.e., from monomer to dimer, that the changes from dimer to trimer are small, and that at the level of a trimer there is conformational flexibility suggests that one cannot expect in aqueous solution a polynucleotide with a single rigid spatial configuration. Recent examination of the anatomy of tRNA vis-à-vis polynucleotide flexibility by Rich et al. (1979) supports this thesis where they find the molecule adopting unusual conformations associated with chain extension, with changes in direction of the polynucleotide chain or with the accommodation of other bases which intercalate into the chains.

Acknowledgments

The authors thank Professor B. Pullman and Dr. C. Giessner-Prettre for their help in the calculations.

Supplementary Material Available

Oligomerization shifts (Table III) and contributions from ring current and diamagnetic and paramagnetic anisotropy effects to the projected shifts (Table V) (2 pages). Ordering information is given on any current masthead page.

References

Arnott, S., Dover, S. D., & Wonacott, A. J. (1969) *Acta Crystallogr., Sect. B 25*, 2192.

Cheng. D. M., & Sarma, R. H. (1977) *Biopolymers 16*, 1687.

Cheng, D. M., Dhingra, M. M., & Sarma, R. H. (1978) *Nucleic Acids Res. 5*, 4399.

Dhingra, M. M., & Sarma, R. H. (1979) in *Stereodynamics of Molecular Systems* (Sarma, R. H., Ed.) p 3, Pergamon Press, New York.

Dhingra, M. M., Sarma, R. H., Giessner-Prettre, C., & Pullman, B. (1978) *Biochemistry 17*, 5815.

Evans, F. E., & Sarma, R. H. (1976) *Nature (London) 263*, 567.

Everett, J. R., Hughes, D. W., Bell, R. A., Alkema, D., Nielson, T., & Romaniuk, P. J. (1980) *Biopolymers* (in press).

Ezra, F. S., Lee, C. H., Kondo, N. S., Danyluk, S. S., & Sarma, R. H. (1977) *Biochemistry 16*, 197.

Giessner-Prettre, C., & Pullman, B. (1976) *Biochem. Biophys. Res. Commun. 70*, 578.

Giessner-Prettre, C., & Pullman, B. (1977) *J. Theor. Biol. 65*, 171.

Giessner-Prettre, C., & Pullman, B. (1978) *Jerusalem Symp. Quantum Chem. Biochem. 11*, 161.

Hall, R. H., & Khorana, H. G. (1955) *J. Am. Chem. Soc. 77*, 1871.

Kondo, N. S., Ezra, F. S., & Danyluk, S. S. (1975) *FEBS Lett. 53*, 213.

Ladner, J. E., Jack, A., Robertus, J. D., Brown, R. S., Rhodes, D., Clark, B. J. C., & Klug, A. (1975) *Nucleic Acids Res. 2*, 1623.

Lee, C. H., Ezra, F. S., Kondo, N. S., Sarma, R. H., & Danyluk, S. S. (1976) *Biochemistry 15*, 3627.

Michelson, A. M. (1966) *Biochim. Biophys. Acta 114*, 460.

Neidle, S. (1979) *Nature (London) 279*, 474.

Quigley, G. J., Seeman, N. C., Wang, A. H. J., Suddath, F. E., & Rich, A. (1975) *Nucleic Acids Res. 2*, 2329.

Rich, A., Quigley, G. J., & Wang, A. J. (1979) in *Stereodynamics of Molecular Systems* (Sarma, R. H., Ed.) p 315, Pergamon Press, New York.

Sarma, R. H., Ed. (1979) *Stereodynamics of Molecular Systems*, Pergamon Press, New York.

Sarma, R. H., & Danyluk, S. S. (1977) *Int. J. Quantum Chem., Quantum Biol. Symp. 4*, 269.

Stout, D. D., Mizuno, H., Rubin, J., Brennan, T., Rao, S. T., & Sundaralingam, M. (1976) *Nucleic Acids Res. 3*, 1111.

Sussman, J. L., & Kim, S. H. (1976) *Biochem. Biophys. Res. Commun. 68*, 89.

Verheyden, J. P. H., & Moffat, J. G. (1964) *J. Am. Chem. Soc. 86*, 1236